

ITC 3/53 Information Technology and Control Vol. 53 / No. 3 / 2024 pp. 724-735 DOI 10.5755/j01.itc.53.3.36432	A Semi-supervised Generative Adversarial Network Algorithm for Alzheimer's Disease Analysis	
	Received 2024/02/23	Accepted after revision 2024/05/20
	HOW TO CITE: Yan, J., Gui, R., Liang, H. (2024). A Semi-supervised Generative Adversarial Network Algorithm for Alzheimer's Disease Analysis. <i>Information Technology and Control</i> , 53(3), 724-735. https://doi.org/10.5755/j01.itc.53.3.36432	

A Semi-supervised Generative Adversarial Network Algorithm for Alzheimer's Disease Analysis

Jian Yan, Renzhou Gui, Hao Liang

College of Electronic and Information Engineering, Tongji University, Shanghai, China

Corresponding author: Renzhou Gui, rzgui@tongji.edu.cn

Currently, the study of Alzheimer's disease (AD) imaging classification based on deep learning has become a research hotspot. But due to the characteristics of AD samples with lack of labels and small samples, there are some difficulties in classifying task. In this paper, Semi-supervised generative adversarial network algorithm is designed. Firstly, an improved generative network algorithm is designed to extract and inherit features related to AD, while ignoring non-disease related variations of AD to the disease to generate new samples, achieving sample size expansion and data enhancement. Then, an unsupervised clustering algorithm is constructed to generate sample clustering categories, so that the new samples have different types of AD brain atrophy labels. The test results show that the algorithm achieves good and stable clustering on the real sample test dataset (ADNI-1), and identifies four types of AD brain atrophy patterns. The Calinski-Harabasz Index of the algorithm is calculated about 2388, and the Silhouette Coefficient Index is calculated about 0.588. With these cluster indexes, the algorithm has better clustering performance than traditional clustering methods such as k-means. These research results will contribute to further studying the classification of AD, and contribute to the analysis and diagnosis of the etiology of AD.

KEYWORDS: Deep learning Alzheimer's disease, Cluster analysis, Generative Adversarial Networks, Unsupervised learning.

1. Introduction

Alzheimer's disease (AD) is a neurodegenerative disease commonly seen in the elderly population. AD can cause serious damage to the patient's brain, leading

to emotional and behavioral impairments. Deep patients may also face sleep disorders and circadian disturbances [1]. Emotional disorders in AD patients

may further evolve into apathy, manifested as impairment of social cognition and weakening and loss of behavioral motivation [6]. Ultimately, it leads to visual spatial skill deficits and loss of language ability in AD patients, and affects procedural memory [9].

AD is a neurodegenerative disease, and its pathogenesis is not yet fully understood. In recent years, the rapid development of neuroimaging technology has provided new means for the study of AD. Magnetic resonance imaging (MRI) is a non-invasive, high-resolution imaging technique widely used in the diagnosis and evaluation of AD. AD is a neurodegenerative disease characterized by functional changes caused by structural changes in the patient's brain, and the accumulation of these changes can lead to structural changes. This structural change is well reflected in structural magnetic resonance imaging (sMRI). Therefore, in the classification of AD based on imaging, sMRI images are the most widely used [13]. The study of sMRI classification can help doctors screen patients earlier and more accurately, and can also delve into the subtype patterns and pathogenesis of AD [11, 14]. With the development of science and technology, many deep learning (DL) technologies have the advantage of processing big data, which makes them start to apply sMRI data classification [12]. Due to limitations in the principles of neuroimaging technology, it is difficult to compare data from different models of magnetic resonance imaging devices and data from the same model with different parameters, resulting in a scarcity of sMRI samples. At the same time, sensitive clinical data and difficulties in data sharing among research institutions further limit the scale of sMRI data. The limitations, such as a small sample size, lack of annotation, and cumbersome annotation process, fail to meet the requirements of deep learning for training data. Consequently, the performance of the training model is also subpar. Therefore, the small sample problem has always been a challenge that needs to be overcome in the field of neuroimaging. Increasing training samples to achieve data augmentation can effectively be solved the small sample problem.

In this paper, the semi-supervised generative adversarial network with clustering function algorithm is designed, which combines supervised and labeled generative adversarial networks with unsupervised and unlabeled clustering algorithm. This model extracts features and expands the sample size of the

dataset by generating adversarial networks part based on publicly available sMRI data. Then the clustering part is used to cluster several subtypes in the progression of AD, that is, to classify brain atrophy patterns. By expanding the sample size and ignoring changes unrelated to the disease, better and disease related results can be obtained in the final clustering analysis, improving classification accuracy. Through the identification of different brain atrophy patterns, modern medicine may be able to further explore the pathogenesis of AD and the treatment of AD.

2. Data and Preprocessed

2.1. sMRI Dataset

The publicly available datasets commonly used in AD imaging research include Alzheimer's disease neuroimaging initiative (ADNI) and open access series of imaging studies (OASIS) and other databases. The MRI dataset is derived in this paper from the ADNI dataset which is an AD related data that is publicly available to all scientists around the world. Its creation goal is to detect and screen AD at the earliest possible stage, and determine methods for tracking disease progression with biomarkers. By applying new diagnostic methods at the earliest possible stage, which is also the most effective stage of intervention, it helps to advance AD intervention, prevention, and treatment. The ADNI database has four stages of research, namely ADNI-1, ADNI-GO, ADNI-2, and ADNI-3. The four research stages have different goals. The main research objective of ADNI-1 is to develop biomarkers as outcome indicators for clinical trials. So far, ADNI has recruited a total of 1317 women and 1426 men as participants to provide relevant data. This article randomly selects partial T1 weighted imaging sMRI as the dataset in the ADNI database for clustering analysis of brain atrophy patterns in AD. T1 weighted imaging is chosen can better observe the tissue structure of the brain. The sample is randomly selected, without considering the influence of covariates such as age and gender, in order to identify a more universal and common pattern change between subtypes of AD disease, and to assist in further analysis and research on AD disease.

Two datasets were selected in this paper. The training dataset used is based on the MUSE [3] software

processing method proposed by Yang et al., who artificially created a training dataset to demonstrate the ability of the algorithm model. The dataset used for the test was sMRI sample data from T1 weighted imaging of 600 cognitively normal individuals (cn) and 600 patients (pt) randomly selected from the ADNI-1 database. The sample is randomly selected, without considering the influence of covariates such as age and gender, in order to identify a more universal and common pattern change between AD subtypes, and to assist in further analysis and research on AD.

2.2. sMRI Data Pre-processed

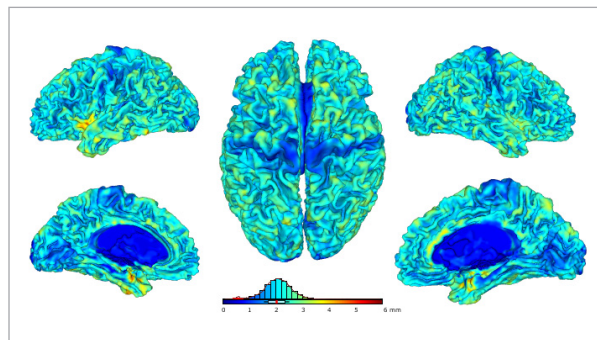
Due to the fact that the sMRI data in the dataset is in 3D format, the program runs quite slowly when using sMRI data as the input dataset for neural network training. The sMRI data contains redundant information unrelated to changes in AD. Therefore, the sMRI data is preprocessed before used, including calibration and localization, removal of non brain structures, image segmentation, smoothing, and other processing steps. In the step of image segmentation, the brain is divided into gray matter, white matter, and cerebrospinal fluid. The process of AD has different impacts on these three parts of the brain. After preprocessing, the ROI (Region of Interest) data are obtained by dividing the sMRI 3D image into regions of interest (ROI Matrix).

According to the template, the trained ROI data contain 254 ROI regions in gray matter, white matter and cerebrospinal fluid. To save the running time of the algorithm, the gray ROI data are selected that are most commonly used in classification. The patient data are compared with cognitively normal data, and some ROI region data which are similar in cognitively normal data and patient data are screened out. Finally, 145 ROI regions are obtained as training regions. The test dataset is randomly selected brain data from 1200 participants in the ADNI-1 database, of which 600 are cn data and 600 are pt data. By repeatedly preprocessing sMRI data, a corresponding dataset can be obtained, which will be used to cluster the brain atrophy patterns of real AD patients. The pre-processed sMRI data is shown in Figure 1.

In the paper, three specific atrophy patterns were randomly introduced on the basis of cn data as training datasets to verify the clustering ability of the model. Its format is also a $1200 (=600+600) * 145$ ROI dataset.

Figure 1

The pre-processed sMRI data



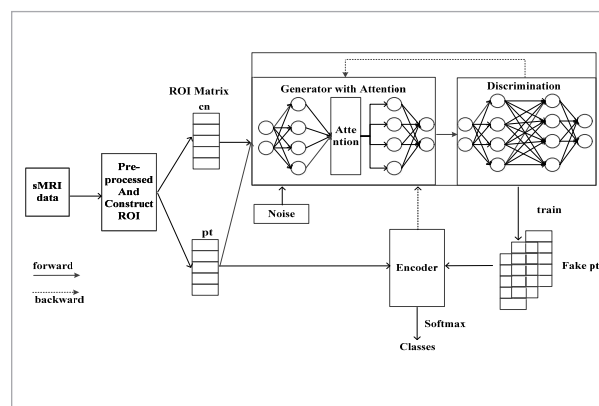
3. Methodology

3.1. Semi-supervised Generative Adversarial Network

The semi-supervised generative adversarial network is a structure based on the combination of generative adversarial network (GAN) algorithm and clustering algorithm model. The function of the GAN network is to expand the sample size, while the clustering network extracts the most fundamental data features through autoencoder and achieves clustering. The 145 ROI data inputs are enhanced by generating adversarial network data for training the encoder clustering network. The trained encoder network performs clustering analysis on pt data to obtain a clustering analysis of AD brain atrophy patterns. The algorithm flowchart is shown in Figure 2.

Figure 2

The algorithm flowchart



The loss function of network is defined as in equation:

$$L = Loss_{GAN} + \lambda Loss_{AE} + \mu L1. \tag{1}$$

The loss function(L) not only includes the losses caused by the GAN network structure ($Loss_{GAN}$) that generates the data, but also the losses caused by the clustering network encoder ($Loss_{AE}$). The L1 is Lasso regularization. The λ and μ are hyperparameter. The loss function value not only reflects the authenticity of the generated pseudo pt data, but also reflects the clustering effect of the model.

3.2. Improved Generative Adversarial Network

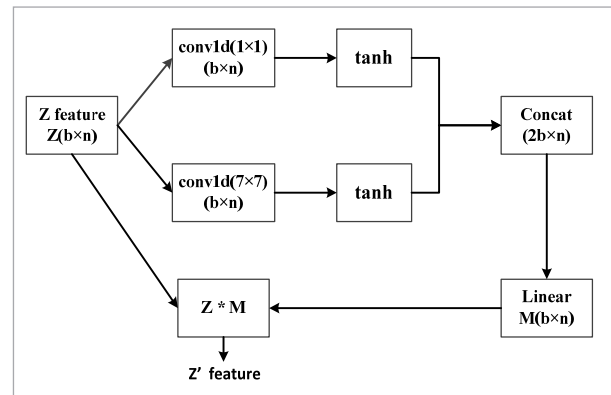
The GAN is a framework that generates models through adversarial process estimation without prior probability modeling, and can learn the true sample distribution [5]. The GAN consists of a generator and a discriminator, both of which are composed of neural networks. However, the GAN has problems such as unstable training, mode collapse, and unclear training level. In order to solve these problems, Arjovsky et al. proposed the wasserstein generative adversarial network [2]. The wasserstein generative adversarial network (WGAN) measures the distribution difference between two samples using wasserstein distance on the basis of traditional GAN. The WGAN networks belong to unsupervised learning. It uses random noise as the input of generator G, which has the advantage of making the network more applicable. However, the method of starting from noise also has the disadvantage of starting to extract and capture the features of the target distribution without any foundation. Therefore, the time required for final convergence is long, and the final effect remains to be discussed.

The AD dataset includes pt data and cn data, and those different data can be used as classification labels. The random noise is considered as input to generator G in the GAN network, while the random noise with cn data characteristics (cn data features are added to random noise through the neural network) is considered as input x to generator G the improved GAN network (iGAN), and pt data is used as input y to discriminator D. The research objective is to classify the patterns of brain atrophy in AD patients, and the classification work is unsupervised. If the non-disease related variations m are the characteristic value of the cn data, it

also exists in the pt data [15]. There are implicit n patterns (disease related variations) in the patient data of AD, that is, the pt data has m+n characteristic values. A linear mapping relationship will first be captured in the improved GAN network, and simulated pt data(y_{fake}) will be generated through this mapping. The goal of discriminator D is to distinguish y and y_{fake} as much as possible. The y_{fake} as the training data input for the clustering network can extract and recognize features related to AD disease n as the basis for clustering, thus achieving the goal of ignoring changes unrelated to the disease. It is assumed that there are non-disease parameters on the images of real dataset (pt) besides the disease features to be extracted. At the same time, there is a background dataset (cn) containing no-disease features, which also contains information unrelated to disease features. In this case, generator G can achieve the effect by extracting and inheriting the features of the background dataset.

In order to obtain relevant information between ROIs in feature extraction, an attention mechanism is added to the generator G. Attention mechanism model structure is shown in Figure 3.

Figure 3
Attention mechanism model structure



The attention model is divided into short attention branches and long attention branches, both of which learn global features at different levels in parallel to obtain information about global features. Afterwards, the short attention branch and the long attention branch are combined to obtain comprehensive global features. Finally, the global features are combined with the original input branch to attach the influence of global weights to the noise.

The loss function of network is defined as in equation:

$$Loss_{iGAN}(P_r, P_\theta) = \sup_{\|f\|_L \leq 1} E_{x \sim P_r}[f(g(x))] - E_{z \sim P_\theta}[f(g(z))]. \quad (2)$$

Among them, $\|f\|_L$ is the Lipschitz constant of function f , and the function g is a clustering operation. P_r and P_θ are two sample distributions. P_g is a joint distribution of P_r and P_θ . λ is the weight of gradient penalty. The wasserstein distance in the iGAN is not a measure of the distance between the distribution of simulated data and real data, but rather a measure of the distance between the cluster center of the pt sample data within the clustered category and the distribution of the simulated dataset within the clustered cluster center. The problems such as vanishing gradients can be avoided while the gradient penalty is added. The higher the wasserstein distance, the better the clustering effect. By limiting the wasserstein distance to enhance the clustering effect, iGAN network can adapt more efficiently in AD classification, improve training efficiency and accuracy, and achieve the expansion of AD sample data and preliminary classification of samples.

3.3. Clustering

Clustering algorithm is a kind of unsupervised learning algorithm utilized for drawing inferences from the datasets containing input data without any labeled responses. The k-means clustering method is a common unsupervised clustering method. There are many evaluation indicators for measuring clustering effectiveness. For example, Sum of Squared Error (SSE), Calinski Harabasz (CH), Silhouette Coefficient (SC) Davies Boundin Index (DBI), Adjusted Rand index (ARI). The AD atrophy pattern is an unsupervised clustering algorithm that can be evaluated using the first four indicators. The ARI indicator is used as a clustering evaluation indicator, which can be achieved by repeatedly training multiple models through the same clustering network and comparing the clustering results of multiple models. The ARI index not only evaluates the clustering effect, but also shows the stability of model training.

Auto-encoder (AE) is used as the clustering part of the semi-supervised generative adversarial network to achieve the clustering function [10]. The AE is a common unsupervised learning model in deep learning, often used in clustering analysis tasks. It can be

used for feature extraction without the need for manually extracting feature values [8].

The network structure of clustering is implemented in the paper by combining the encoder part of traditional autoencoders with the softmax function. The formula for softmax is as follows:

$$softmax(x) = \frac{e^{x_i}}{\sum_{j=1}^n e^{x_j}}. \quad (3)$$

Among them, n is the clustering category. Due to the unsupervised training of the model, n needs to be set. The parameter x is the hidden layer vector obtained by the encoder.

The loss function of network is defined as in equation:

$$Loss_{AE} = \sum_{n=1}^N \|z' - f(g(x, z))\|^2. \quad (4)$$

Among them, f is the reconstruction function for the autoencoder. g is generator G . z is the noisy of generate G , and z' is the result of f .

The clustering model is trained through data enhanced sample data generated by the improved GAN network. The original real (pt) data is analyzed using this clustering model to achieve higher accuracy and efficiency.

4. Experiment and Discussion

The purpose of the semi-supervised generative adversarial network constructed in the paper is to capture brain atrophy patterns in AD. The change in atrophy pattern does not mean the progression of the disease over time, nor does it mean a prediction of the patient's condition, but simply a classification and judgment of the category to which they belong. Therefore, atrophy patterns are some constant and implicit patterns throughout the entire AD process. In the common areas of brain atrophy in AD diseases, the degree of atrophy is artificially enhanced or weakened, and the pattern characteristics are enhanced. The dataset was used with three patterns of atrophy as the training set to train the clustering effect of the model.

The operating environment is as follows: CPU is Intel (R) Core (TM) i7-8565U, GPU is NVIDIA GeForce GTX 1050Ti, memory is 8G, and operating system is Windows10 64 bit operating system.

Adam Optimizer is set as the optimizer, and the learning rate is set to 0.0001. The threshold of Wasserstein distance is set to 0.14, and the loss function loss value of the clustering algorithm is set to be less than 0.002.

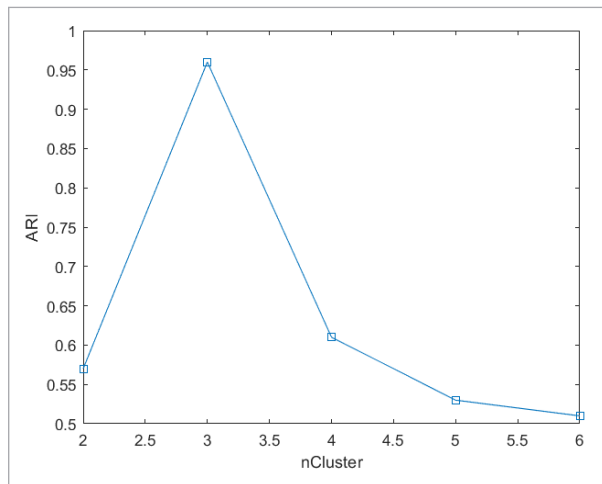
4.1. Analysis of Model Training Effect

The clustering category of AD brain atrophy patterns is unknown, and the clustering method used is unsupervised. Therefore, the number of clustering categories needs to be pre-set. When running the model, the number of cluster categories is set to 2, 3, 4, 5, and 6.

The ARI indicators of clusters with different categories are shown in Figure 4.

Figure 4

ARI indicators for clustering under different categories

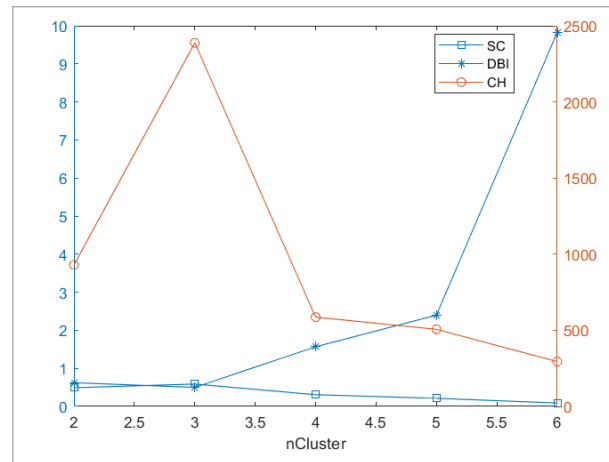


The higher the ARI index, the better the distance stability and training effectiveness of the model. From the graph, it can be seen that setting the number of clusters to 3 is the best clustering method for AD subtypes. Under different categories, the scores of other indicators in the model are shown in Figure 4.

From the Figure 5, it can be seen that the SC score and CH score of 3-cluster are higher than other cluster categories. The DBI value of 3-cluster is lower than other cluster categories. Among them, the higher the SC score and CH core, the better the clustering effect, the smaller the DBI value, the better the classification effect. Thus, it can also be confirmed that the model is the best clustering method for AD subtype classification when the number of clustering categories is set to 3.

Figure 5

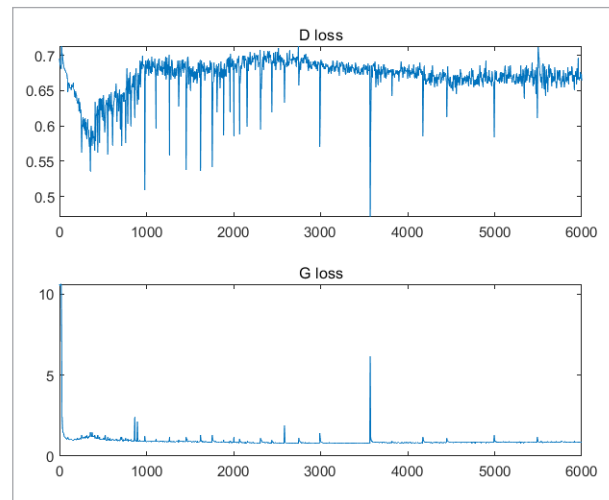
Other indicators of the model



When the number of clustering categories is set to 3, the loss value of model training is shown in Figure 6.

Figure 6

Loss of model training



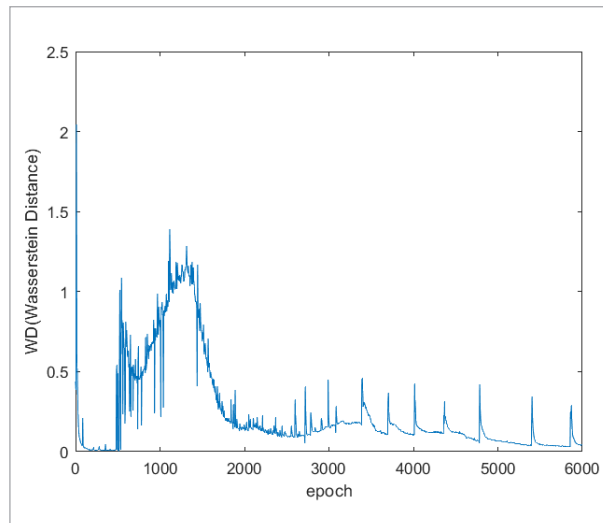
From Figure 6, it can be seen that the loss value of discriminator D increases after reaching the lowest value, and the final value stabilizes between 0.65 and 0.7. This is because generator G was trained first. The loss function of generator G not only includes the losses caused by iGAN structure, but also the losses caused by subsequent clustering network encoders. After 6000 epochs of model training, the semi-supervised generative adversarial network gradually reach stable convergence.

The wasserstein distance reflects the clustering effect more intuitively than the loss function value of generator G. The smaller the distance value, the better the clustering effect of model training. Wasserstein distance variation of clustering centers is shown in Figure 7.

From Figure 7, it also can be seen that the wasserstein distance increases after reaching the lowest value,

Figure 7

Wasserstein distance of cluster center distribution



and finally it is stabilized at a low value as the model gradually converges.

Through the variation of the loss function value and the wasserstein distance, it can be seen that with the training of the network model, the semi-supervised generative adversarial network constructed ultimately achieved good results in data enhancement and clustering analysis, and achieved relatively successful clustering results. The final result is that the best clustering method is divided into 3 categories, which is consistent with the three patterns artificially created by the dataset. It indicates that the model can perform well in clustering analysis of heterogeneous AD sample data, and can effectively identify potential disease-related features in the sample dataset. The clustering center of a category is used to analyze and compare three types of clustering patterns. The cluster center is shown in Figure 8.

Among them, ROI is the horizontal axis, and volume is the vertical axis. It can be clearly seen that the cluster centers of different cluster categories

Figure 8

Cluster centers of pt samples

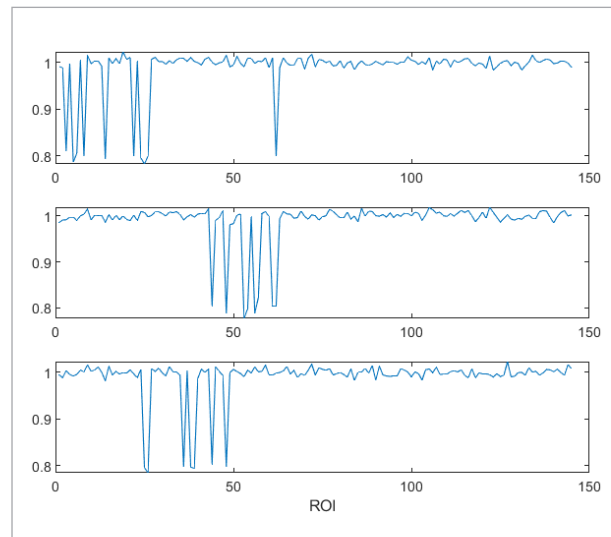


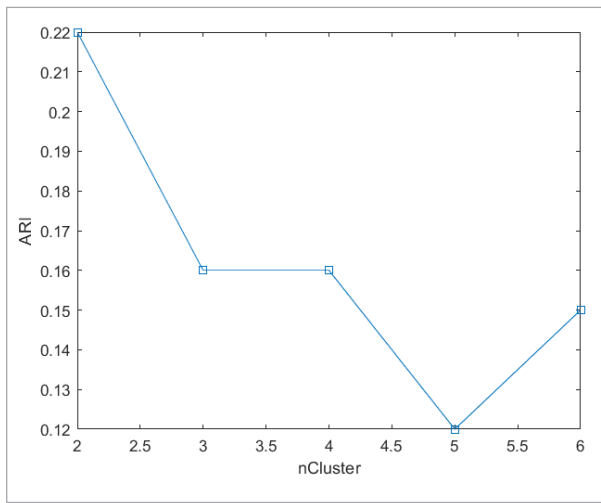
exhibit varying degrees of atrophy at different ROI positions. The first type of cluster mainly undergoes atrophy in areas such as the nucleus accumbens, amygdala, and hippocampus of the brain, indicating the loss of neurons related to emotional and olfactory functions. The clustering features of the second type of cluster mainly demonstrate the brain atrophy of patients in areas such as the anterior orbital gyrus, indicating a decline in olfactory related functions. The third type of cluster exhibits atrophy in the temporal and occipital lobes, indicating a decline in visual and other related functions. The cluster centers of the three clusters all demonstrate the decline of memory and other functional related abilities in patients with AD.

4.2. Analysis of Model Testing Results

The test data is 1200 sMRI data randomly selected from the ADNI-1 database (<https://adni.loni.usc.edu/data-samples/access-data>)(600 for cn data and 600 for pt data). These sMRI data are preprocessed to generate 1200 ROI data. The 1200 ROI data are as model input. The number of cluster categories is set to 2, 3, 4, 5, and 6. The ARI indicators of clusters with different categories are shown in Figure 9.

From Figure 9, it can be seen that the best number of categories should be 2. The standard deviation of ARI reaches ± 0.23 when 2 categories, which indicating a

Figure 9
ARI of different categories under test set data

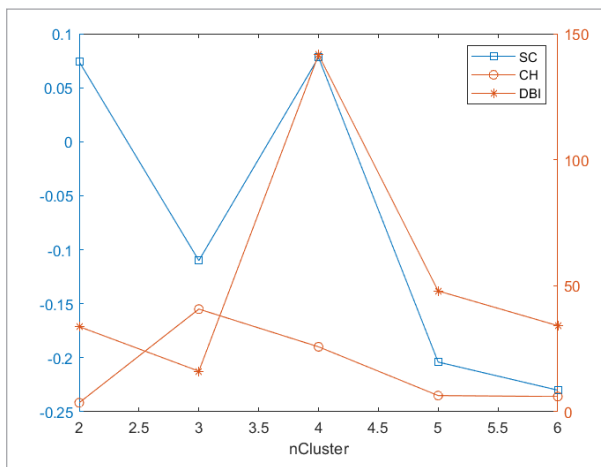


certain difference between the four trained models. However, when the number of ARI score categories is 4, the standard deviation is ± 0.03 , making the model more reliable.

To enhance the generalization ability of the model, other clustering indicators will be selected as enhanced validation of the clustering results. Under different categories, the scores of other indicators in the model are shown in Figure 10.

The SC value reflects intra class cohesion, The DBI value reflects inter class distance of different cate-

Figure 10
Other indicators in different categories under test set data



gories, and CH value measures the first two simultaneously. From Figure 10, it can be seen that 4-cluster and 2-cluster have higher SC values. The DBI absolute value of 4-cluster is lower than other cluster categories. Thus, the best number of categories should be 4. It is the same result obtained by the ARI indicator.

When the clustering categories are 2 and 4, the atrophy below the average value of each cluster center is shown in Figures 11-12.

Figure 11
Atrophyin cluster centers with nCluster=2

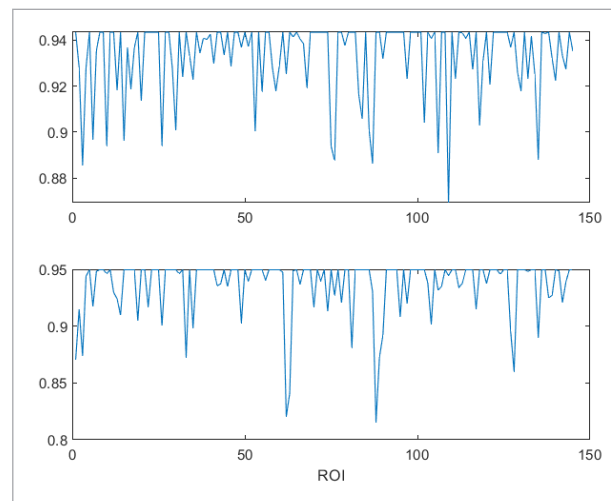
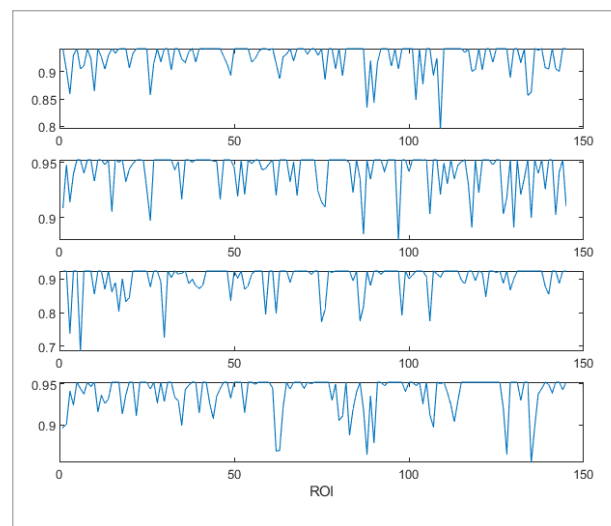


Figure 12
Atrophyin cluster centers with nCluster=4



When the number of clustering categories is 2, the clustering results are divided into two categories, without reflecting the specificity of the atrophy pattern. When the number of cluster categories is 4, the brain regions with an ROI of around 100 in the first cluster show specific atrophy. The second type of cluster shows atrophy in multiple brain regions. The first 10 ROI regions of the third cluster shows atrophy. The fourth type of cluster showed atrophy between 50 and 100, and between 100 and 150. The first, third, and fourth types of atrophy patterns represent three subtypes of brain atrophy changes that occur in the early stages of AD, while the second type of atrophy pattern represents brain atrophy in the later stages of AD. Therefore, category 4 was ultimately selected as the classification method for the test set. Research on classification will reveal more information on further AD.

4.3. Comparison with k-means Clustering Method

The clustering category is set to 3, and both models are trained on the training set. By comparing the calculation methods of various clustering indicators, the results are shown in Table 1.

Table 1

Index Evaluation of Two Clustering Methods

Method	<i>SC</i>	<i>DBI</i>	<i>CH</i>
This paper	0.588	0.500	2388.174
K-means	0.070	3.429	38.449

Through the comparison of clustering indicators, the semi-supervised generative adversarial network has obvious advantages over k-means in clustering, which is largely attributed to the enhancement of the sample data by the added generative adversarial network.

4.4. Comparison of Clustering Effects Before and After Data Enhanced

The sample data and the sample data enhanced by semi-supervised generative adversarial network are trained on CNN clustering networks respectively. The training effect is shown in Figures 13-14.

From two figures, the accuracy network training on the original sample is 87.88%, while the accuracy network training on enhanced by semi-supervised generative adversarial network is 96.54%. The data set is enhanced

Figure 13

Original sample network training curve

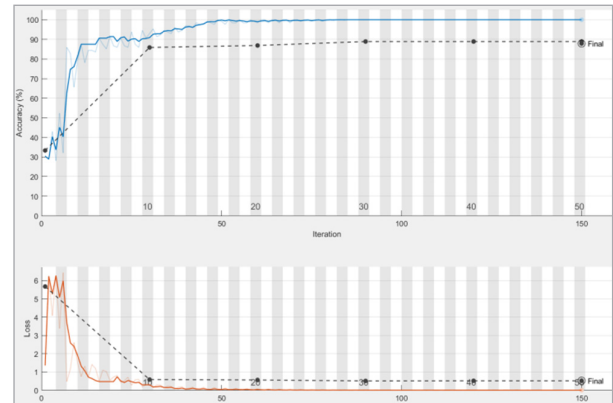
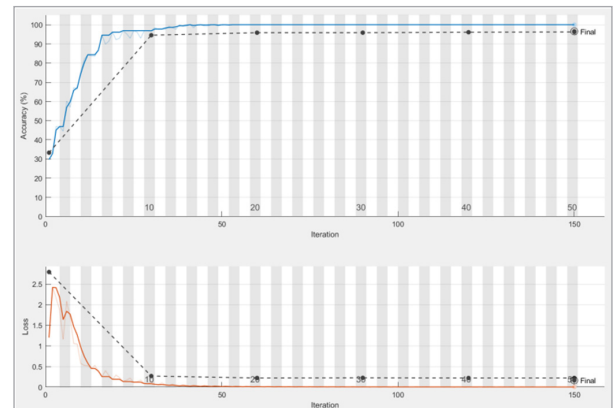


Figure 14

Enhanced sample network training curve



by semi-supervised generative adversarial network has a significant improvement effect on network training.

4.5. Analysis with Supervise Mechine Learning Combinations

The label data are generated based on clustering output in the paper, and used as input for supervised machine learning such as SVM [4], GaussianNB, KNN, Decision Tree [7] to retrain. The purpose of retraining the results through other machine learning methods can further reduce the number of features used in clustering. By selecting unique or shared ROI regions between different patient subtypes to compare a specific subtype or subtypes, it is discovered whether there may be commonalities behind AD heterogeneity. The classification effect of four methods is shown in Figure 15, The accuracy of four methods is shown in Table 2.

Figure 15

The classification effect of four methods with unique features

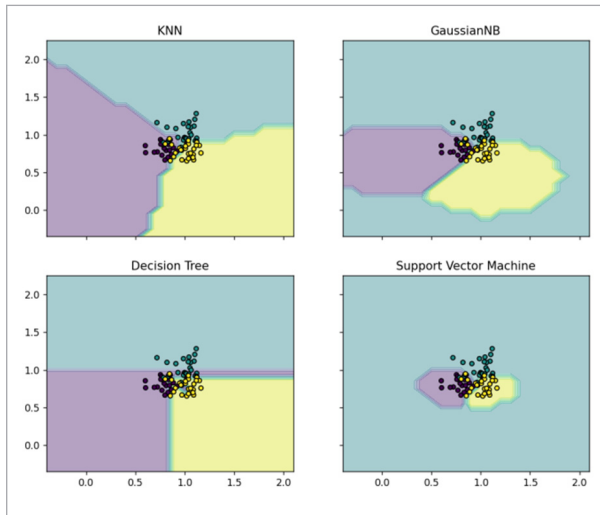


Table 2

The accuracy of four methods with unique features

Method	KNN	GaussianNB	Decision Tree	SVM
Accuracy	0.81	0.84	1.00	0.79

The selected ROI region data is classified based on common features of AD subtypes. The classification effect is shown in Figure 16, The accuracy is shown in Table 3.

Figure 16

The classification effect of four methods with common features

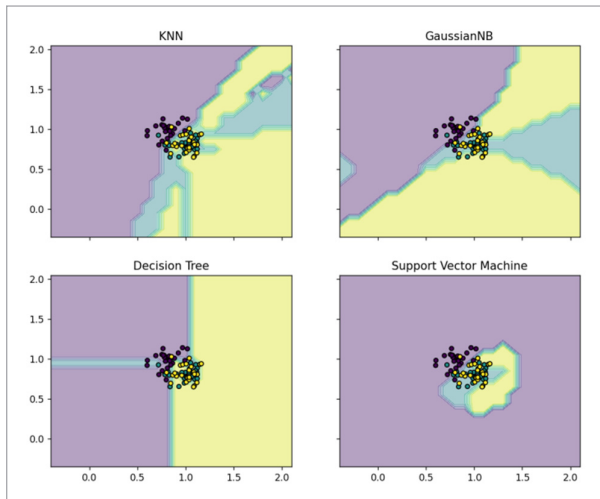


Table 3

The accuracy of four methods with common features

Method	KNN	Gaussian-NB	Decision Tree	Support Vector Machine
Accuracy	0.75	0.69	1.00	0.69

From Figure 15, it can be seen that when selected ROI regions with common features for different AD subtypes, the clustering results show an overlap of sample data for the two subtypes. According to further clustering analysis results, it can be seen that the AD subtypes summarized by clustering on brain images have special and common features.

Through further classification and analysis of the clustering results by semi-supervised generative adversarial network, it can be more clearly seen that AD has an impact on brain atrophy. AD has different effects on different regions of the brain, and there are also heterogeneity differences among different individuals. The study of AD disease changes in different people will help doctors to personalized treatment for patients, while the potential common rules of AD disease in different people will help to study the pathogenesis.

5. Conclusions

This paper proposes a semi-supervised generative adversarial network to solve the problem of small sample size and lack of labels in the sMRI dataset for AD effectively. Firstly, the sMRI data is preprocessed before used, and the ROI data is obtained by dividing the preprocessed sMRI data into ROI matrix. Secondly, the model is designed to extract features and expand the sample size of the dataset by iGAN, and ignore parts unrelated to disease features. The model has a self-attention mechanism, which has multiple levels of attention to help capture important global and local features. Finally, the clustering category is obtained through the algorithm clustering section. The loss function value of the network includes the loss value of the generated adversarial network part and the loss value of the clustering network part, so that the loss function not only reflects the authenticity of the generated pseudo data, but also reflects the clustering effect of the model. The experimental results show that The semi-supervised generative adversarial network has achieved

good and stable clustering performance on the ADNI-1 sample dataset, and obtained real four types of brain atrophy patterns in AD. The CH value and SC value of the algorithm are calculated about to 2388 and 0.588, and the DBI value is calculated about to 0.5. Compared with the traditional k-means clustering method, the results showed good and stable clustering performance. Through further clustering analysis of machine learning, it can be seen that AD subtypes have characteristics and common features in brain imaging.

In the future, in order to improve the accuracy and generalization ability of classification models, semi supervised generative adversarial networks will be combined with deep classification models to train

data. And further research will be conducted on high-precision classification and finer ROI segmentation methods of supervised learning to explore AD related biomarkers, obtaining new insights and promoting the development of AD disease assisted diagnosis research.

Competing Interests

The authors have no relevant financial or non-financial interests to disclose.

Acknowledgements

The authors acknowledge the National Natural Science Foundation of China (Grant: 41827807).

References

1. Amidfar, M., Garcez, M. L. Kim, Y.-K. The Shared Molecular Mechanisms Underlying Aging of the Brain, Major Depressive Disorder, and Alzheimer's Disease: The Role of Circadian Rhythm Disturbances. *Progress in Neuro-Psychopharmacology and Biological Psychiatry*, 2023, 123, 110721. <https://doi.org/10.1016/j.pnpbp.2023.110721>
2. Arjovsky, M., Chintala, S., Bottou, L. Wasserstein Generative Adversarial Networks. *Proceedings. Mlr. Press; PMLR*. 2017. <https://proceedings.mlr.press/v70/arjovsky17a.html>
3. Doshi, J., Erus, G., Ou, Y., Resnick, S. M., Gur, R. C., Gur, R. E., Satterthwaite, T. D., Furth, S., Davatzikos, C. MUSE: MUlti-atlas Region Segmentation Utilizing Ensembles of Registration Algorithms and Parameters, and Locally Optimal Atlas Selection. *Neuro Image*, 2016, 127, 186-195. <https://doi.org/10.1016/j.neuroimage.2015.11.073>
4. Fan, Z., Xu, F., Qi, X., Li, C., Yao, L. Classification of Alzheimer's Disease Based on Brain MRI and Machine Learning. *Neural Computing and Applications*, 2019, 32(7), 1927-1936. <https://doi.org/10.1007/s00521-019-04495-0>
5. Goodfellow, I., Pouget-Abadie, J., Mirza, M., Xu, B., Warde-Farley, D., Ozair, S., Courville, A., Bengio, Y. Generative Adversarial Nets. *Neural Information Processing Systems; Curran Associates, Inc.* 2014. https://papers.nips.cc/paper_files/paper/2014/hash/5ca3e9b122f61f8f06494c97b1afccf3-Abstract.html
6. Johansson, M., Stomrud, E., Johansson, P. M., Svenningsson, A., Palmqvist, S., Janelidze, S., Van Westen, D., Mattsson-Carlsson, N., Hansson, O. Development of Apathy, Anxiety, and Depression in Cognitively Unimpaired Older Adults: Effects of Alzheimer's Disease Pathology and Cognitive Decline. *Biological Psychiatry*, 2022, 92(1), 34-43. <https://doi.org/10.1016/j.biopsych.2022.01.012>
7. Karami, V., Nittari, G., Traini, E., Amenta, F. An Optimized Decision Tree with Genetic Algorithm Rule-Based Approach to Reveal the Brain's Changes During Alzheimer's Disease Dementia. *Journal of Alzheimer's Disease*, 2021, 84(4), 1-8. <https://doi.org/10.3233/JAD-210626>
8. Lu, M., Zhou, B., Bu, Z. Attention-Empowered Residual Autoencoder for End-to-End Communication Systems. *IEEE Communications Letters*, 2023, 27(4), 1140-1144. <https://doi.org/10.1109/LCOMM.2023.3242281>
9. Neha, Parvez, S. Emerging Therapeutics Agents and Recent Advances in Drug Repurposing for Alzheimer's Disease. *Ageing Research Reviews*, 2023, 85, 101815. <https://doi.org/10.1016/j.arr.2022.101815>
10. O'Shea, T., Hoydis, J. An Introduction to Deep Learning for the Physical Layer. *IEEE Transactions on Cognitive Communications and Networking*, 2017, 3(4), 563-575. <https://doi.org/10.1109/TCCN.2017.2758370>
11. Prajjwal, P., Marsool, M. D. M., Inban, P., Sharma, B., Asharaf, S., Aleti, S., Gadam, S., Al Sakini, A. S., Hadi,

- D. D. Vascular Dementia Subtypes, Pathophysiology, Genetics, Neuroimaging, Biomarkers, and Treatment Updates along with Its Association with Alzheimer's Dementia and Diabetes Mellitus. *Disease-a-Month*, 2023, 69(5), 101557. <https://doi.org/10.1016/j.disease-a-month.2023.101557>
12. Raju, M., Thirupalani, M., Vidhyabharathi, S., Thilagavathi, S. Deep Learning Based Multilevel Classification of Alzheimer's Disease Using MRI Scans. *IOP Conference Series: Materials Science and Engineering*, 2021, 1084(1), 012017. <https://doi.org/10.1088/1757-899X/1084/1/012017>
 13. Scelsi, M. A., Napolioni, V., Greicius, M. D., Altmann, A. Network Propagation of Rare Variants in Alzheimer's Disease Reveals Tissue-specific Hub Genes and Communities. *PLOS Computational Biology*, 2021, 17(1), e1008517. <https://doi.org/10.1371/journal.pcbi.1008517>
 14. Tijms, B. M., Teunissen, C. E. Concatenating Plasma P-tau to Alzheimer's Disease. *Brain*, 2021, 144(1), 14-17. <https://doi.org/10.1093/brain/awaa422>
 15. Yang, Z., Nasrallah, I. M., Shou, H., Wen, J., Doshi, J., Habes, M., Erus, G., Abdulkadir, A., Resnick, S. M., Albert, M. S., Maruff, P., Fripp, J., Morris, J. C., Wolk, D. A., Davatzikos, C., Fan, Y., Bashyam, V., Mamouiran, E., Melhem, R., Pomponio, R. A Deep Learning Framework Identifies Dimensional Representations of Alzheimer's Disease from Brain Structure. *Nature Communications*, 2021, 12(1). <https://doi.org/10.1038/s41467-021-26703-z>



This article is an Open Access article distributed under the terms and conditions of the Creative Commons Attribution 4.0 (CC BY 4.0) License (<http://creativecommons.org/licenses/by/4.0/>).